Controls on mesophotic carbonate facies and sediment distribution across the Maltese shelf, central Mediterranean Sea

Or M. Bialik; Giovanni Coletti; Christian Berndt; Mark Schmidt; Aaron Micallef

For more information contact the authors: OMB - obialik@uni-muenster.de, GC - giovanni.coletti@unimib.it, AM - aaron.micallef@um.edu.mt

Controls on mesophotic carbonate facies and sediment distribution across the Maltese shelf, central Mediterranean Sea

Or M. Bialik[1,2*]; Giovanni Coletti[3]; Christian Berndt[4]; Mark Schmidt[4]; Aaron Micallef[5]

1. Institute of Geology and Palaeontology, University of Münster, Corrensstr. 24, 48149 Münster, Germany

2. Dr. Moses Strauss Department of Marine Geosciences, The Leon H. Charney School of Marine Sciences, University of Haifa, Carmel 31905, Israel

3. Department of Earth and Environmental Sciences, University of Milano-Bicocca, Piazza della Scienza 4, 20126 Milano, Italy.

4. GEOMAR Helmholtz Centre for Ocean Research Kiel, Wischhofstraße 1-3, 24148 Kiel, Germany.

5. Marine Geology & Seafloor Surveying, Department of Geosciences, University of Malta, Msida, MSD 2080, Malta.

* Corresponding author

Abstract

Although ~20% of global carbonate occurs on extra-tropical shelves, our understanding of these depositional environments still lags far behind that of tropical carbonate platforms. The Maltese shelf in the central Mediterranean offers an opportunity to study *in situ* facies distribution in a light-dominated extra-tropical carbonate platform and the factors controlling them. The Maltese shelf visually exhibits three main facies: seagrass meadows; sand flats/bedforms and maerl. While visually distinctive, the allochem composition of the sediment does not offer a clear differentiation of all three but rather a gradient. This gradient is marked by increasing grain size with depth, a transition from green to red calcareous algae and an increase in the fraction of low Mg calcite. While some of these features could be explained by changes in light availability, other factors are also in play. Internal waves, currents and baffling by seafloor vegetation appear to play important roles in governing the sedimentary texture and composition across the Maltese shelf. The role of vegetated substrate is of greater importance in Mediterranean C-type carbonate factories and could be an important marker to identify them in the geological record.

Keywords: coralline algae, Malta, maerl, calcareous sand, carbonate factories

Introduction

Carbonate factories represent both the space where biological carbonate sediments are produced and the associations of carbonate-producing organisms (Schlager, 2003; Tucker and Wright, 1990). Given the large fossilization potential of most carbonate-producing organisms, carbonate factories have a massive fossil record that spans most of Phanerozoic, providing a powerful archive for investigating the evolution or our planet (Bosellini and Perrin, 2008; Coletti et al., 2022; Halfar and Mutti, 2005; Kiessling et al., 1999; Kiessling and Flügel, 2002; Perrin and Bosellini, 2012; Pomar et al., 2017). As such, understanding of modern carbonate factories is essential for quality reconstruction of past environmental conditions (Bialik et al., 2023; Westphal et al., 2010).

The two most common shallow-water carbonate factories in the modern ocean are considered to be the T-Type and C-Type factories (Michel et al., 2019; Reijmer, 2021; Schlager, 2005). T-Type carbonate factories (T stands for tropical or "top-of-the-water-column") are the main ones associated with modern carbonate platforms. They develop in warmer waters photic zone by the likes of zooxanthellate corals and calcareous green algae. C-Type carbonate factories (C stands for cool-water or controlled precipitation) span a much larger depth and temperature range with production by bryozoan and coralline algae. Many studies have addressed the depositional environment of C-Type factories (Bassi and Nebelsick, 2010; Basso, 1998; Bosence

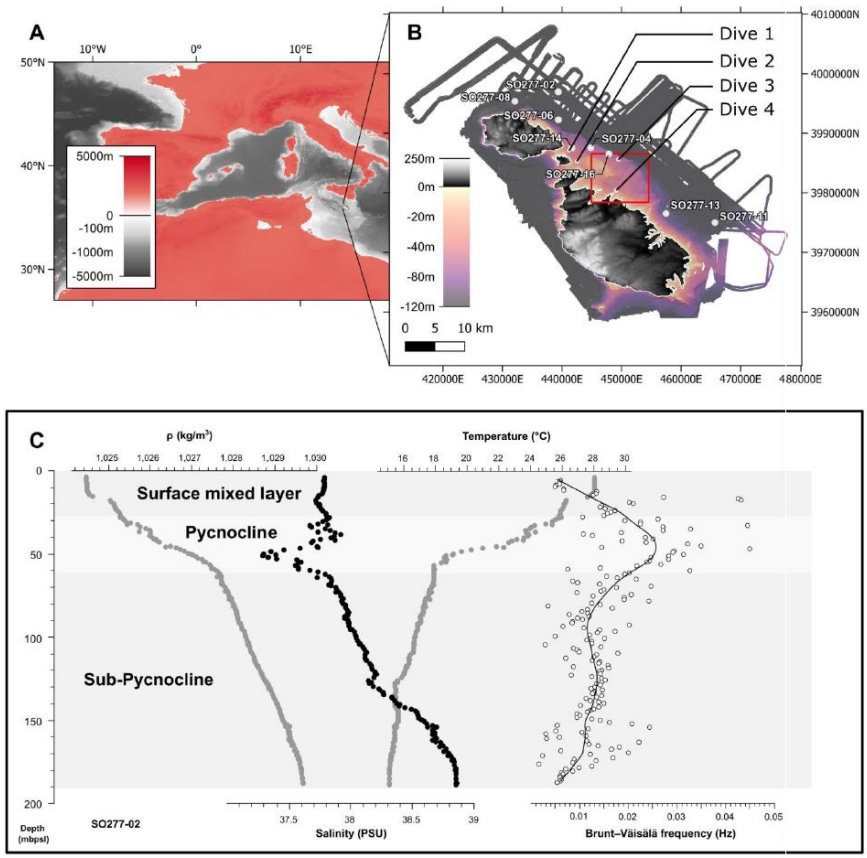

Figure 1: *: A. location map showing the position of the Maltese Archipelago relative to the rest of the Mediterranean. B. Blowup shows the bathymetry for the Maltese shelf and location of the study area (red frame). C. Representative profile of density (ρ), salinity, temperature and Brunt–Väisälä frequencies for the region from CTD station SO277-02.*

and Pedley, 1982; Braga et al., 2012; Coletti and Basso, 2020; De MacEdo Dias and Villaa, 2012; Gaglianone et al., 2017; Halfar et al., 2012; James et al., 2001; Nalin et al., 2006; Nebelsick and Bassi, 2000; Rasser, 2000). Most of these have examined geological deposits, with only a small fraction of the work ground truthing with modern analogs. This stands in stark contrast to T-Type factories, where modern platforms have been extensively studied and their facies are well constrained by modern analogues (Alongi, 1989; Bergman et al., 2010; Gischler, 2006; Gischler et al., 2008; Harris et al., 2015; Smith et al., 1998). This is further complicated by the significant disparity between the nutrient-limited C-Type (n/C-Type) factory present on most oceanic margins and the light-limited C-Type (l/C-Type) factory, which is almost exclusive to the Mediterranean Sea (Laugié et al., 2019; Michel et al., 2019; Reijmer, 2021). The meta-analysis of the distribution of recent allochems indicates that more than distinct factories, modern oceans are characterized by a continuum of carbonate production stretching along an energy gradient, with photozoan production prevailing were the main source of energy is light and heterozoan production prevailing wherever the prevailing source of energy is chemical energy derived from food (Bialik et al., 2023). Such a result is obviously related to the employed data set which is significantly skewed towards the better studied, low latitude carbonate systems.

The benthic communities of the l/C-type factories are exposed to multiple stress vectors, ranging from the large-scale effects of global warming and ocean acidification (Martin and Gattuso, 2009) to local activity such as fishing and trawling (Sciberras et al., 2009). Many of the groups belonging to these benthic community are also still poorly understood and their distribution is mostly unknown (Rindi et al., 2019). However, recent studies undoubtedly proved their sensitivity (Guy-Haim et al., 2020). As such, understanding the environment of these non-tropical communities of carbonate producing organisms and establishing a good sedimentological basis for their exploration is currently crucial.

Works done on n/C-Type carbonate factories in south Australia and the western Atlantic (De MacEdo Dias and Villaa, 2012; Halfar et al., 2012; James et al., 2001) show a significant range of grain sizes and compositional variability. This significant variability is generated by the heterogeneous state of currents, waves and nutrients across these environments. In contrast, there is less knowledge of the spatial variability of these parameters in the Mediterranean Sea (Fichaut et al., 2003), with other factors such as the co-occurrence of baffling elements such as seagrass controlling complexity further enhancing the

complexity of Mediterranean carbonate systems distribution and character (Gaglianone et al., 2017). Our understanding of the spatial distribution of the l/C-Type carbonate factory remains poor, however. Detailed geophysical studies of l/C-Type systems such as the Maltese shelf (Foglini et al., 2016; Micallef et al., 2012) suggest that a combination of depth and seafloor morphology controls the distribution of sedimentary facies in these environments by influencing temperature, light availability and local current regime.

Another element governing this environment is reworking. When producing a large amount of clastic carbonates, many C-type factories develop geometries similar to siliciclastic open shelves (Pomar et al., 2017; Schlager, 2005). As such, some C-type environments are referred to as ramps rather than platforms (Pedley and Carannante, 2006). These geometries are the result of C-type factories producing loose grains rather than a solid framework as the T-type factories. Moreover, differences in diagenetic pathways between the main carbonate minerals in each environment (aragonite in T-type factories; high Mg calcite in C-type factories) result in different hardening patterns. Loose grains are redistributed by oceanic forces, such as currents and waves, as well as metazoans such as fish and echinoderms. The reworking and redistribution of grains can merge and overlap to the effects of depth and seafloor morphology. As a result, facies of and samples from a C-type factory would have a composite signal comprised of a "productivity" signal (governed by light and nutrients) and a "reworking" signal (governed by current and sedimentation rates) (Pomar and Kendall, 2008).

Building upon prior studies on the region that were focused on geophysical exploration or ecology of one group (Ferraro et al., 2020; Lanfranco et al., 1999; Sciberras et al., 2009), the Maltese shelf offers a good setting to improve our understanding of l/C-type carbonate system. Therefore, in order to improve the existing knowledge of non-tropical allochem assemblage, their composition, sedimentological characteristics and paleoenvironmental significance, this study aims at ground-truthing prior geophysical studies on the Maltese shelf, and to delineate the sedimentary facies and their distribution along the shelf. Sediment samples have been collected and analysed providing quantitative data on their sedimentological and mineralogical characteristics and on the abundance of the main carbonate producers. These data are than related to abiotic parameters to better highlight the underlying controls.

Geological setting

The Maltese platform is a shallow water plateau in the central Mediterranean Sea (Figure 1A), surrounding the Maltese archipelago. It is an elevated feature elongated along an NW-SE trend. It is located in the north-eastern part of the Pelagian Block, a plateau representing a remnant of an ancient carbonate platform initially formed in the Tethys Ocean during the Palaeogene (Bishop, 1988; Jongsma et al., 1985; Micallef et al., 2016). As of the Late Miocene, the area experienced uplift driven by a SE-NW directed horizontal shortening as plate convergence between Africa and Europe changed the regional tectonic stress field (Adam et al., 2000; Gutscher et al., 2016; Reuther et al., 1993). Late Pleistocene sedimentation in the region is considered to be mostly aggradational (Osler and Algan, 1999) with the sediment covering the shelf being predominantly sand to gravel size biogenic grains (Micallef et al., 2012). This material is mostly generated on the shelf with limited production of detrital material near shore or supplied from the archipelago (Gatt, 2021).

The range of water depth over the Maltese shelf ranges from 0 to ~100 m. The shelf terminates with a steep margin, resulting in a 10 m to 30 m escarpment. This slope is steeper in the NE and more gradual to the SW. This means that for the most part the shelf is exposed only to the uppermost part of the water column comprising the local surface water and Atlantic Waters (Ben Ismail et al., 2012; Placenti et al., 2013; Warn-Varnas et al., 1999). Oceanographic studies in nearby southern Sicily indicate that surface waves in the region exhibit primarily an east-west main direction with their maximum energy at around 25 m water depth (Iuppa et al., 2015). As there is no available Maltese data at this time and given the small distance, we assume similar behavior in

Malta as well. The regional climate is warm and arid (Galdies, 2011) with low to medium wind intensity. Despite that, extremely powerful storm events are known in the region, transporting massive boulders along the shore and enhancing local coastal erosion (Biolchi et al., 2016; Causon Deguara and Gauci, 2017).

Methods

Study site

The area selected for this study is a sector of the Maltese shelf located northeast of Mellieħa (Għadira) Bay (Figure 1B). This area was selected based on the extensive availability of data for planning sampling activities and the wide range of seafloor types.

Seismic reflection profile

One multichannel seismic reflection profile (P2000_2115_2857), obtained by RV Sonne expedition SO277 (Berndt et al., 2021), was taken into consideration. The profile crosses the shelf across the study area (Figure 2A, right transect). Acquisition was carried out with a 187.5 m-long 120 channel Geometrics GeoEel streamer and two GI-Guns (Generator-Injector Guns) as a seismic source. The data were processed with SeismicUnix and Omega including FX- time migration with a constant velocity of 1500 m/s. The data were visualized and interpreted using the IHS Markit Kingdom software.

Water column parameters

Abiotic parameters of the water mass were retrieved from the dataset of the R/V Sonne expedition SO277 (Berndt et al., 2021). These include CTD data (Supplement 2) collected on the shelf with an attached camera (see Figure 1B for locations). Temperature and salinity data from the CTD casts were binned to 10 second intervals and were used to calculate water density in accordance to the UNESCO formulation (UNESCO, 1981). The Brunt–Väisälä frequency (N) distribution in the water column was calculated using equation 1 (Vallis, 2017):

$$N = \sqrt{\frac{-g}{\rho}\frac{d\rho}{dz}} \quad (1)$$

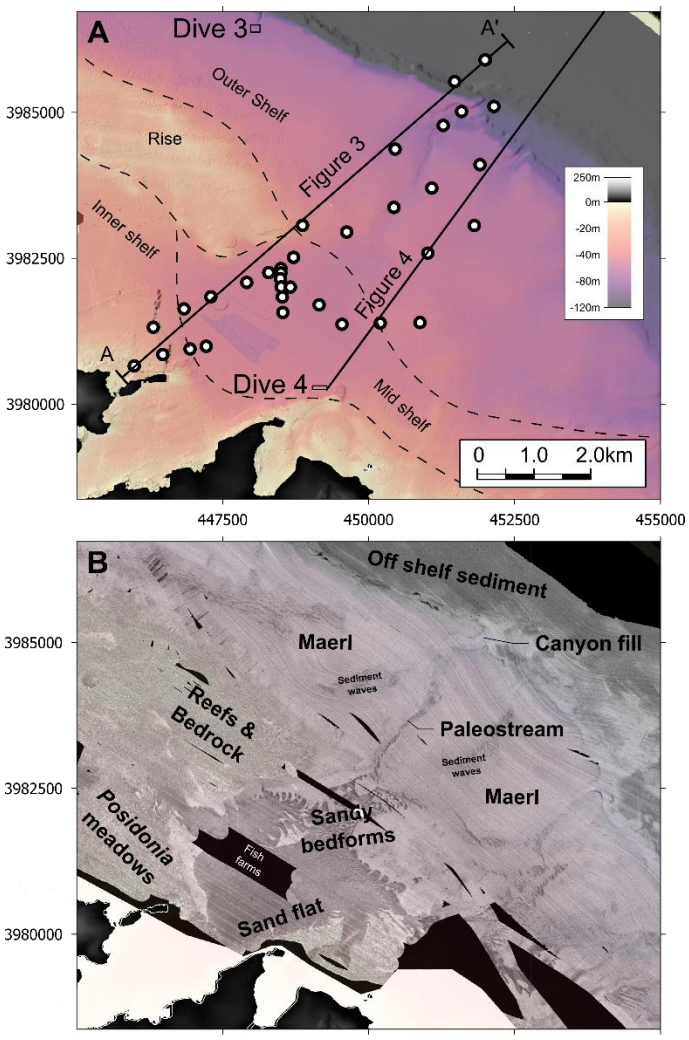

Figure 2: A. bathymetry of the study area showing the locations of the grab samples collected in this study, lines indicate the position of the seafloor profile shown in Figure 3 and seismic profile shown in Figure 4. Differentiation to inner, mid and outer shelf here is based on physical features separating the different zones. B. multibeam backscatter of the study area showing the different bathymetric domains as mapped by prior studies (Berndt et al., 2021; Foglini et al., 2016; Micallef et al., 2012; Prampolini et al., 2018, 2017).

where ρ is the potential density of the fluid, g is the local acceleration of gravity and z is water depth. Data for station SO277-02 is shown in Figure 1C, data from all other stations processed is included in supplementary material (10.6084/m9.figshare.20330490). Wave data were taken from the Mazara del Vallo offshore Sicily (Figure 3).

Seafloor imagery

The video data from the CTD casts was integrated using Agisoft to generate photomosaics. Image quality was too

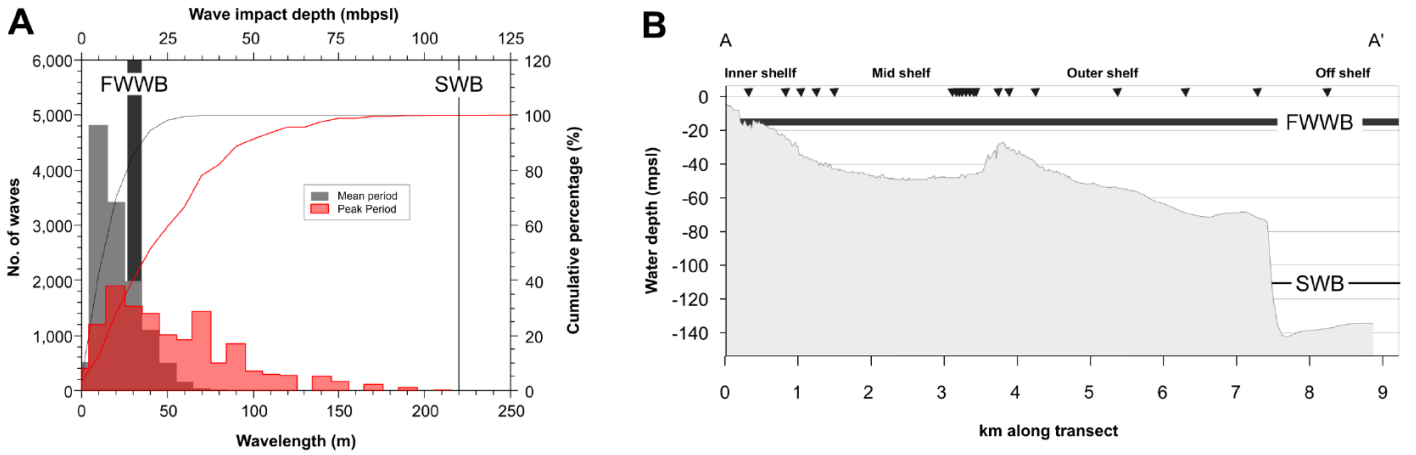

Figure 3: A. wavelength distribution in the Sicily Channel and inferred FWWB and SWB; B. profile of the Maltese shelf in the study area (see Figure 2A) with the depths of the FWWB and SWB.

low to use this information for more than general context. Higher resolution imagery with better spatial coverage was collected by autonomous underwater vehicles (AUV) dives using Girona 500 AUV (IQUA Robotics, Girona, Spain) equipped with a CoraMo mk II Camera which can take up to 2 images per second with a resolution of 12.34MP. Operation and imaging followed operation described in Linke et al. (2015). The imagery collected during these dives was similarly integrated into mosaics. These mosaics were analyzed in the context of the backscatter-based classification to identify the seafloor variability within the sampling error of the sampling tools. Detailed description and analysis of the AUV data is provided in Supplement 1 with summary and key notes provided in the results.

Sample acquisition and processing

A sampling survey was planned using the bathymetric and backscatter data previously described and analyzed (Berndt et al., 2021; Foglini et al., 2016; Micallef et al., 2013, 2012; Prampolini et al., 2018, 2017). Sample positions were selected to cover the full depth range of the shelf and all of the major seafloor facies types identified in Micallef *et al.* (2012). The depth range in the study area, where sampling was permitted, extends from -10 meter relative to present sea level (mpsl) to -140 mpsl (Figure 2A). This area includes (from SW to NE) *Posidonia* meadows; sand flats; reefs and exposed bedrock; ranges of sandy bedforms; maerl; patches of sediment waves; a paloechannel which opens to a canyon (sediment filled) and off shelf sediments (Figure 2B). The sandy bedforms and sand flats both reside within a local basin on the shelf, which was suggested to have been a paleo-alluvial plain (Micallef et al., 2013; Prampolini et al., 2017).

Sampling was carried out in the end of August 2021 aboard the service vessel Gold Finder using an Evenco (Auckland, New Zealand) Shipek grab with a 3000 mL scoop volume. The estimated error on location for each station is ~20m (Figure 2A, Table 1). Samples were transferred from the grab to plastic bags onboard. With return to the port an aliquot of each sample was washed with fresh water over a 63µm mesh. Both the washed and unwashed splits were allowed to air dry until fully dry before any further step was undertaken.

Fully dried samples were photographed and initially described by visual observation. Following that, a detailed description of size and components was carried out under the microscope (Supplements 3, 4). The main components present in each sample were first evaluated in a semi-quantitative fashion (D – Dominant, only component is most view fields; A – Abundant, present in large amount in each view field; C – Common, present in any view field; F – Few, present in some view fields; P – Present, only individual specimen found in all view fields surveyed). Every texture of every sample was also named in

accordance to the modified Dunham classification (Embry and Klovan, 1971; Lokier and Al Junaibi, 2016). Mineralogical determination was carried out using X-Ray diffraction (XRD) for bulk powdered sample. Analysis was carried out using a Rigaku MiniFlex 600 benchtop X-ray diffractometer (30kV/10mA from 3° to 70° at 0.05° increments by point detector) with a Cu target X-ray source. The relative abundance of carbonate species was estimated using the relative intensity ratio methods (Hubbard and Snyder, 1988).

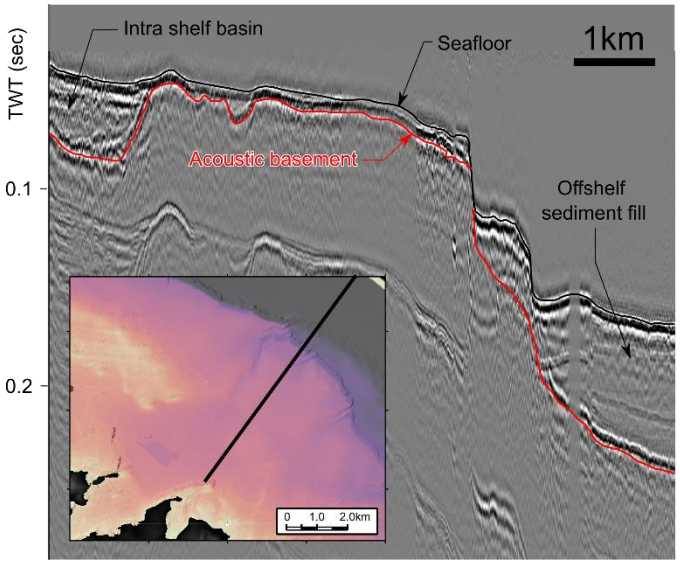

Figure 4: Seismic profile across the Maltese shelf (see inset and Figure 2A). Seafloor and acoustic basement are delineated. Sediment accumulation across most of the shelf is very thin, thickening in the SE intra-shelf sand basin and off shelf to the NE.

Following this phase, thin sections were prepared for selected samples and processed according to standard procedures (Flügel, 2010). Quantitative evaluation of constituents was carried out using point counting (Supplement 5) with detailed component description. Since grain size ranges extended into the gravel size, grain size analysis was done optically. Multiple view fields of each sample were collected and individual grain size were measured using the ImageJ software (Rasband and Contributors, 2021). At least 500 measurements (or all grains present) were collected for each sample. Statistical analysis of the assemblages was carried out following the approach and method outlined in Bialik et al. (2021). All values for both visual and thin sections analysis are available as 10.6084/m9.figshare.20330490.

Results

Seismic reflection profile

The sedimentary cover over most of the Maltese shelf is relatively thin in most places although there are sediment-filled pockets. The thickest of which appears to be the intrashelf basin in the southwest of the study area (Figure 2) which appears to hosts ~20m of sediment fill (Figure 4) compared to a few m at most for the rest of the shelf. In the off-shelf area, however, a more significant sediment accumulation is found, exceeding 30m above the acoustic basement (Figure 4).

Water column structure

The upper 200 m of the water column in the study area consists of three main intervals (Figure 1C, Supplement 2): 1. a surface mixed layer between 0 and ~25 m below present sea level (mbpsl) marked in summer by high temperatures (>26°C); 2. a pycnocline that overlaps with the thermocline and is marked by variable salinity between ~25 and ~60mbpsl; 3. A sub-pycnocline water mass as of ~60 mbpsl marked by increasing density and salinity paired with decreasing temperatures. The maximum Brunt–Väisälä frequencies (ranging between 0.03 and 0.05 Hz) overlaps with the pycnocline whereas below it frequencies are between 0.01 and 0.02 Hz.

Seafloor imagery

Detailed imagery of the seafloor (see Supplement 1 for more information) shows that the main types of seafloor morphology highlighted by low-resolution techniques actually consists of a complex mosaic of multiple sedimentary features. An exception to this pattern seems to be represent bythe sand flats area where photographs (Figure 5A) showed a relatively uniform character composed of biogenic sand with algal material and echinoids. In the seagrass domain, where surveyed in detail, the seafloor resulted to be covered by small patches of seagrass (*Posidonia oceanica*) surrounded by biogenic sand (Figure 5B). This biogenic sand forms bedforms of various

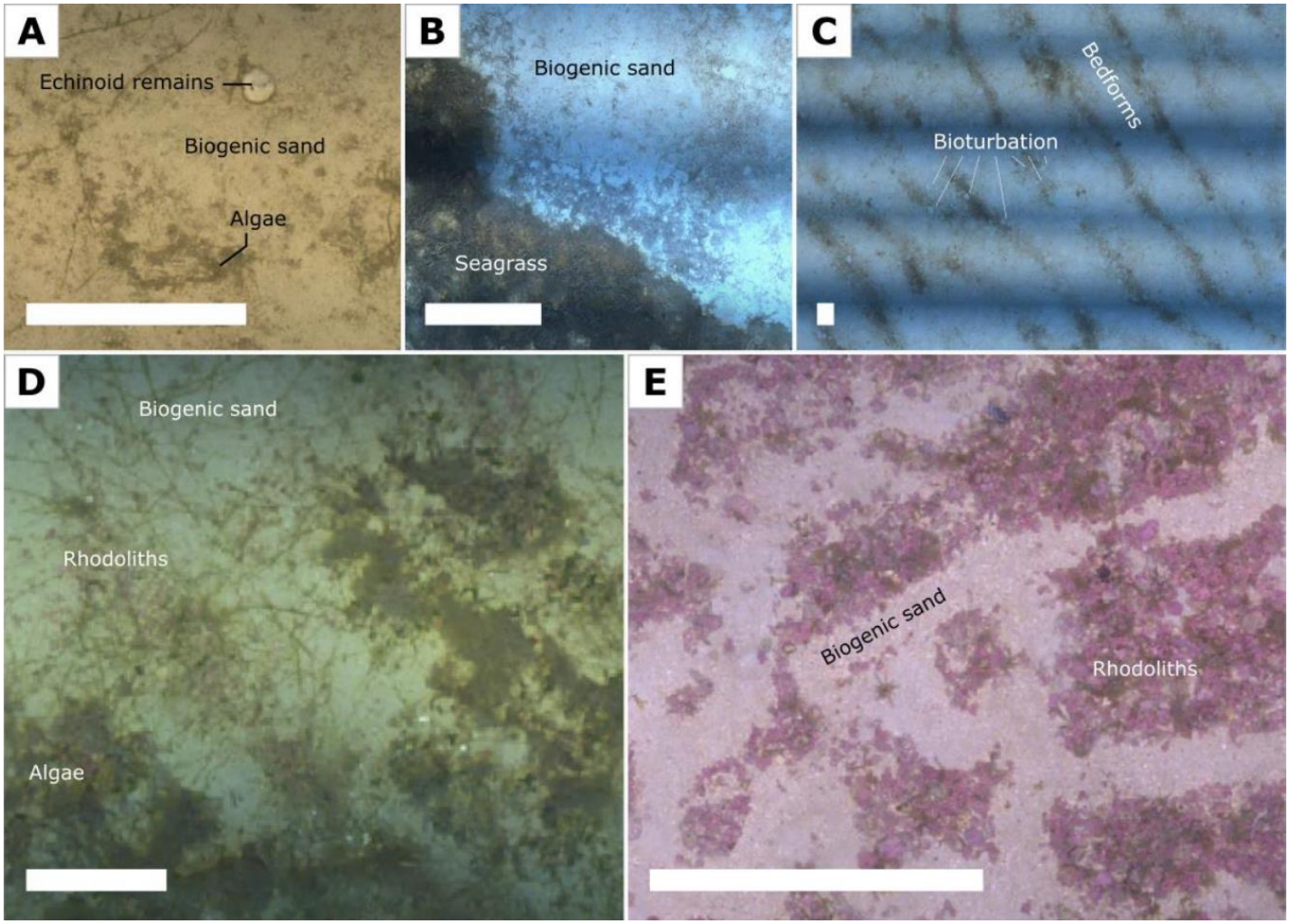

Figure 5: Composite mosaics of seafloor imaging of the maltase shelf (see Figure 1 for locations) showing different characters the seafloor (see Supplement 1 for more information). A. biogenic sand with echinoid remains (Dive 4); B. interface between biogenic sand and seagrass (Dive 2); C. sandy bedforms (Dive 2); D. clumps of flashy algae with rhodoliths and calcareous sand (Dive 1); E. rhodoliths accumulations (Dive 3).

sizes, oriented generally with a strike of NW-SE (Figure 5C) in all locations where they were mapped. In some locations, the bedforms are punctuated by resurfacing, that is to say that the seafloor has been turned over or cleared of biofouling, which appears to be bioturbation (Figure 5C). In the maerl domain, more variety was observed. In shallow water accumulations of coralline algal branches occur, locally interspersed with patches or clumps of fleshy algae (Figure 5D). In deep water there are less fleshy algae and a higher density of coralline algae, the latter also displaying a stronger color (Figure 5E). The rhodoliths are also aligned, developing NW-SE striking bedforms.

Sediment constituents

All samples collected and analyzed within this study were poor in silt (0% to 5.5%) with most of the grains in the sand size (higher than 90% in 22 out of 33 samples) or gravel. The mean grain size ranges between 0.2 and 21.6 mm (mean=2.8±5.6 mm, n=33), with a standard deviation ranging between 0.1 and 11 mm (mean=2.1±3.3 mm, n=33), skewness ranges between 0.3 and 14.6 (mean=3.9±2.7, n=33), With the exception of two samples (samples 29 and 30), all samples exhibit a positive skewness. Mean grain size, standard deviation, %sand or %gravel do not exhibit any correlation to water depth or distance from shore. Skewness exhibits a weak nonlinear correlation to both water depth ($r=-0.43$, $p=0.01$) and distance from shore ($r=-0.45$, $p<0.01$)

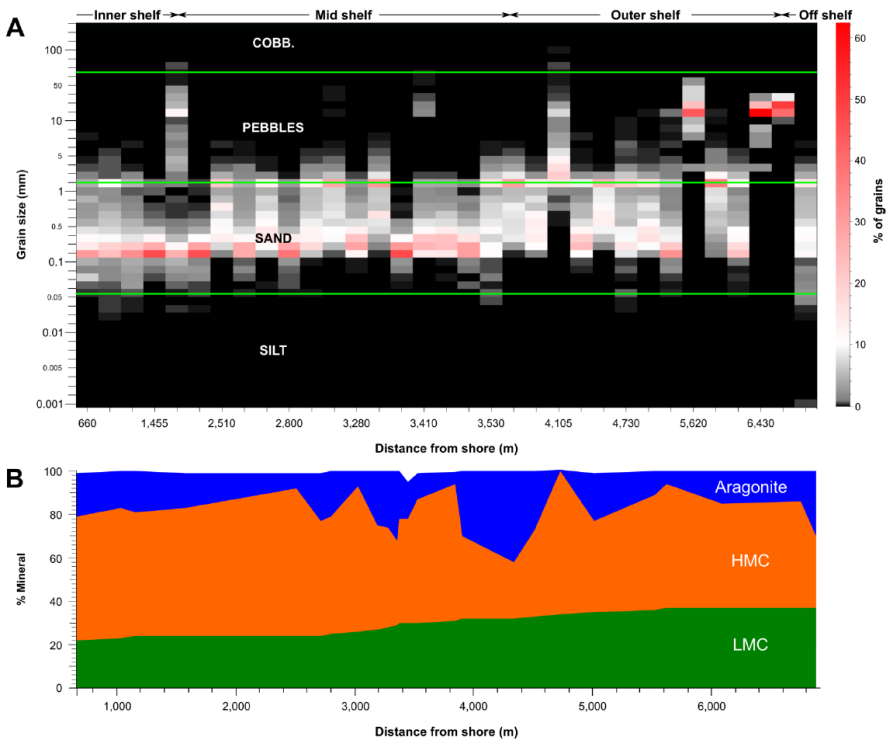

Figure 6: Distribution of sediment parameters across the shelf. A. Grain size distribution along gradient away from shore. B. carbonate mineral ratios across the shelf along distance from shore.

whereas log skewness increases inversely to both. On the shelf, %silt was higher in shallower water and closer to shore, whereas %gravel is higher in the most distal sites (Figure 6a).

When applying the updated Dunham classification of sedimentary texture (Embry and Klovan, 1971; Lokier and Al Junaibi, 2016), shelf samples classify as grainstone, poorly washed grainstone, floatstone with a grainstone matrix or rudstone. Under visual inspection, the most common components in these were few to abundant unidentified bioclasts, either pale or dark brown in color, present to dominant coralline algae. These occur as branches or nodules of various size, when larger than 1 cm (clearly visible in the submarine imaging) considered here as rhodoliths, with the latter being the most common), present to common benthic foraminifera and present to few bryozoan and echinoid fragments. Bivalves, gastropods, pteropods, serpulids, fragments of *Halimeda* were found in some samples. Sample 9 consisted almost entirely of *Cladocora*. Both the rudstone and floatstone textures are primarily due to presence of coralline algae, and occur mostly farther away from shore. The distribution of the component does not exhibit any clear trend, although foraminifera are somewhat more common in shallower waters, *Halimeda* in the mid shelf and coralline algae are somewhat more common in the outer shelf. Seagrass remains and/or fleshy green algae were found in 13 samples in water depths between 28 and 69 mbpsl. Seagrass remains were found in poorly washed grainstone to floatstone with grainstone matrix samples, while fleshy algae were found with all sedimentary textures. Both seagrass and fleshy algal remains were found in only two samples, both consisting of grainstones (Supplement 3).

The principal mineralogies of the sediments (in order of abundance) are high Mg calcite (HMC), aragonite and low Mg calcite (LMC). No significant amount of clays or quartz was detected in the samples. The HMC ranges between 43% and 93% (mean=63±11%, n=26); Aragonite between 1% and 42% (mean=19±10%, n=26) and LMC between 7% and 25% (mean=18±4, n=26). The fraction of LMC increases with distance from shore (Figure 6b) and is present in all samples, including samples comprised purely of coralline algae. Aragonite is more abundant in the mid-shelf than in the nearshore or outer shelf.

Detailed analysis and point counting of the thin sections confirm the initial visual analysis with unidentifiable bioclastic fragments (0% to 67.3%, mean=29.4±18.5%, n=26) and coralline algae (0.3% to 95%, mean=41.6±30.7%, n=26) being the most abundant components (Figures 7A & B). Unidentifiable bioclastic fragments probably represent finely comminuted remnants of benthic foraminifera (mainly miliolids) (Figure 7C). Coralline algae are mainly represented by encrusting Corallinales and Hapalidiales (including *Phymatolithon calcareum*) (Figure 7D), while Sporolithales are extremely rare. Articulated coralline

algae also occur in samples close to the coast (Figures 7E & F). Benthic foraminifera are also abundant (0% to 37%, mean=13±11%, n=26), especially close to the coast. They are mainly represented by small miliolids (*Triloculina*, *Quinqueloculina*, *Spiroloculina*) (Figure 7F & G), encrusting miliolids (nubeculariids) and small rotaliids (*Ammonia*, *Elphidium*, *Asterigerinata*, *Cibicides*) (Figure 7C & E); large rotaliids are less common and mainly represented by specimens of *Planorbulina* (Figure 7H). Echinoderms are also relevant and are mainly represented by elements of irregular echinoids close to the coast (Figure 7I) and by regular echinoids more offshore. Mollusks (mainly gastropods and bivalves) commonly occur in most samples and they can be locally relevant (Figure 7J). *Halimeda*, bryozoans, serpulids and ostracods contributions are usually minor (Figure 7K & L).

It is apparent that the abundance of several constituents exhibits a near linear decline with distance from shore (and similarly to water depth), notably unidentifiable bioclastic fragments ($r=-0.47$, $p=0.02$), echinoids ($r=-0.47$, $p=0.02$), rotaliids ($r=-0.58$, $p<0.01$) and miliolids ($r=-0.62$, $p<0.01$). The abundance of *Halimeda* correlates to water depth ($r=-0.55$, $p<0.01$) but not to distance from shore ($r=-0.31$, $p>0.05$). Coraline algae exhibits an opposite trend to these, increasing with depth ($r=0.60$, $p<0.01$) and distance from shore ($r=0.66$, $p<0.01$). The abundance of mollusks, bryozoans, serpulids, ostracods or textulariids does not exhibit any correlation to water depth or distance from shore. However, mollusk abundance is higher in the mid shelf. No parameter appears to correlate with the intensity of the seafloor backscatter in a statistically significant fashion.

Several components exhibit strong correlations to each other, e.g. the abundance of echinoids correlates both to the presence of miliolids ($r=0.71$, $p<0.01$), rotaliids ($r=0.88$, $p<0.01$) and unidentifiable bioclastic fragments ($r=0.72$, $p<0.01$). To further elucidate these relations, multi-variant analysis was carried out using detrended correspondence analysis (DCA) and non-metric multidimensional scaling (nMDS) using Bray-Curtis indices. Axis 1 and 2 of the analysis accounts to eigenvalues of 0.41 and 0.06, respectively. The principle loading on axis 1 of the DCA (Figure 8A) is the coralline algae (RCA) to negative and everything else with positive loading. On axis 2 the negative loading is by coralline algae, miliolids, rotaliids, serpulids and sponge spicules. The result of the nMDS analysis (Figure 8B) has a stress of 0.02, the loading on coordinate 1 is positive for coralline algae, molluscs, bryozoans and textulariids, negative for anything else; coordinate 2 has positive loading for echinoids, unidentified bioclasts, mollusks and textulariids, negative for anything else.

Reworked grains are prevalent in the investigated sediments (Figure 7M-O). They consist of either bioclasts displaying extensive borings and micritization (up to becoming unrecognizable, Figure 7M) or of lumps of poorly lithified material (packstones to floatstone textures) (Figure 7N). Wherever bioerosion and micritization do not obliterate original structures entirely, reworked assemblages seem to have a composition similar to that of pristine assemblages. The overall abundance of reworked grains seems to increase with increasing distance from the shoreline, with most coralline-algal-rich samples dominated by reworked material. This can be clearly noticed in the rhodoliths-dominated, sample 26, where thin crusts of relatively fresh coralline algae grow over cores consisting of micritized coralline algae whose structures are almost completely obliterated (Figure 7O).

Discussion

Sedimentary facies of the Maltese shelf

The Holocene sedimentary cover atop the Maltese shelf is, for the most part, a thin veneer accumulated atop the glacial truncation (Figure 4). This resulted in many terrestrial features such as paleochannels and local basins (Figure 2B) punctuating the shelf (Micallef et al., 2013). Prior acoustic mapping of the seafloor (Micallef et al., 2012), 2013) identified that these relict features host relict facies which currently occur elsewhere on the shelf, organized in distinct

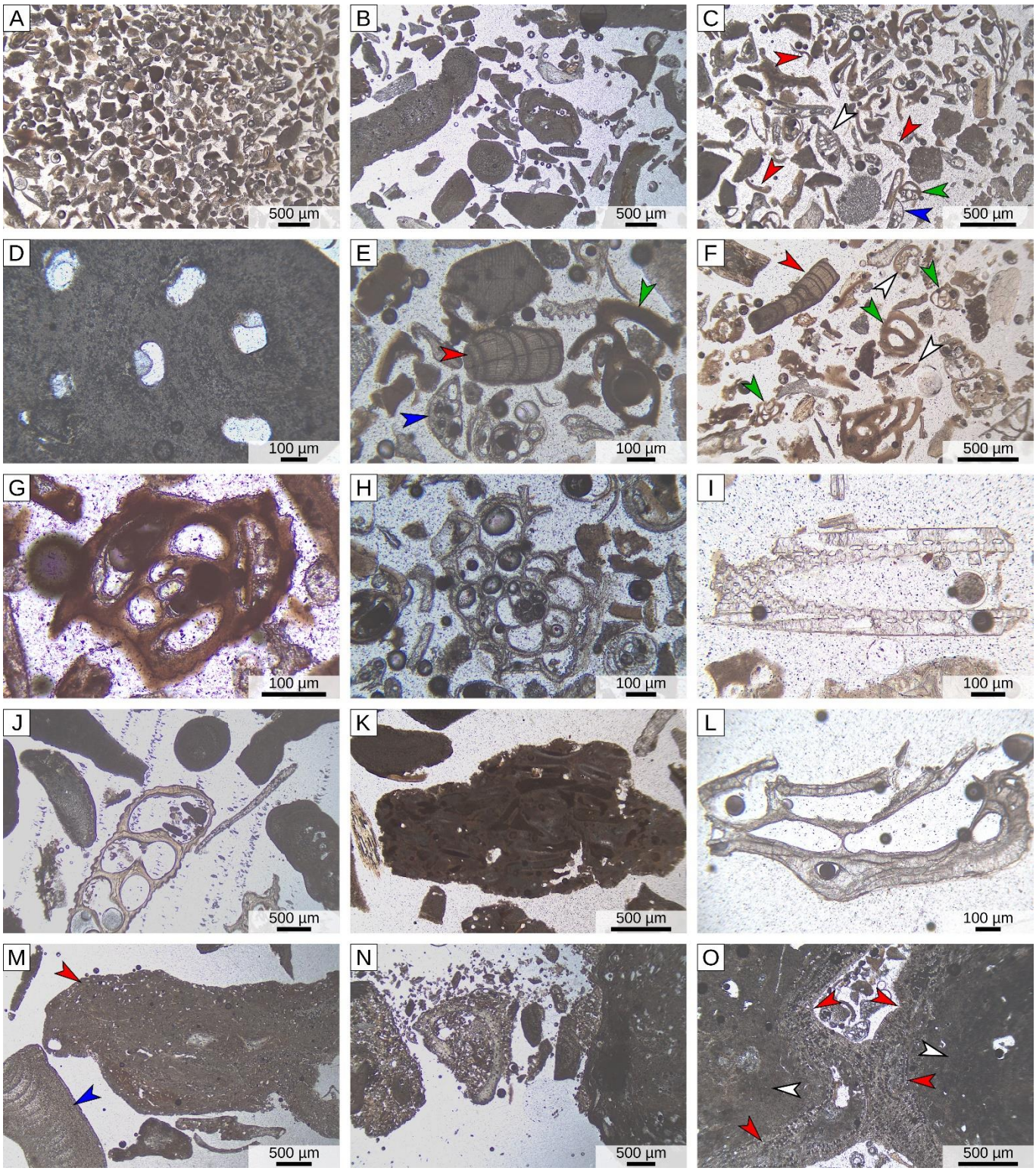

Figure 7: A. Sample 4, dominated by finely comminuted and well sorted unidentifiable bioclastic fragments. B. Sample 23, dominated by coralline algae. C. Sample 18, dominated by finely comminuted and well-sorted bioclastic fragments, several of these fragments are fragments of miliolids (red arrowheads); white arrowhead= Elphidium; green arrowhead= small miliolid; blue arrowhead= Cibicides. D. Sample 24, Phymatolithon calcareum a coralline alga belonging to the Hapalidiales order. E. Sample 18, a fragment of an articulated coralline alga (red arrowhead); blue arrowhead= small rotaliid, possibly Asterigerinata; green arrowhead= small mioliolid. F. Sample 2 displaying common small miliolids (green arrowhead) and small miliolids fragments (white arrowheads); red arrowhead= articulate coralline alga. G. Sample 15, Triloculina. H. Sample 13, Planorbulina. I. Sample 22, irregular echinoid spine. J. Sample 12, rich in pristine coralline algae and molluscs. K. Sample 7, Halimeda. L. Sample 21, bryozoans. M. Sample 19 characterized by common reworked grains including coralline algal fragments displaying extensive microborings (red arrowhead); blue arrowhead= pristine coralline alga. N. Sample 28, dominated by reworked grains of poorly lithified floatstone. O. Sample 26, a coralline algal nodule consisting of a thin outer layer of recent coralline algae (red arrowheads) growing over a nucleus consisting of micritized coralline algae (white arrowheads).

facies belts. Our analysis of the seafloor imaging shows these three main types of facies occurring on the analysed area of the Maltese shelf (Figure 9): a proximal facies with seagrass and fleshy algae (Figure 5B) with a sedimentary texture corresponding to packstone to grainstone; an intermediate facies (mostly occurring in relict troughs) dominated by calcareous sand, withlesser amount of fleshy algae (Figure 5A), and with sedimentary texture corresponding to grainstone to floatstone; an outer shelf facies dominates by rhodoliths (maerl, Figure 5E), with sedimentary texture corresponding to grainstone to rudstone. Additionally, there is an off-shelf facies with a sedimentary texture corresponding to packstone. The off-shelf domain also hosts an additional facies in the form of coralligenous buildups in the south east of the Island (Bialik et al., 2022), which are not present in the north western shelf examined here.

These high order classifications do not translate directly to the sedimentary composition of the sediment. The sediment composition across the inner and mid shelf, corresponding to the seagrass meadows and the sand flats, exhibit the same allochems (benthic foraminifera, molluscans, echinoids, *Halimeda*, bryozoans, coralline algae and large amount of unidentifiable bioclasts). The abundance of most of these allochems diminishes with distance from shore irrespective of the acoustic facies, with some components (e.g. *Halimda*) being dependent only on water depth. In the ordination space, the samples from the seagrass meadows cannot be clearly differentiated from those of the sand flats, in the DCA analysis (Figure 8A), whereas some separation can be observed in the nMDS (Figure 8B). Seagrass and sand flat samples are instead clearly differentiated from maerl samples. In grain size and minerology (Figure 6) some differentiation between these Seagrass and sand flat samples is present, with the more proximal samples hosting some silt-sized fraction that is almost entirely absent in the mid shelf samples dominated by sand flats material. Inner shelf samples are also characterized by higher HMC abundance relative compared to the mid shelf, which exhibits higher aragonite content than the other two regions.

Seafloor vegetation plays an important role in the retention of fine grained material on Mediterranean shelves (Hendriks et al., 2010). Through physical befalling and reduction of current velocities (Fonseca and Koehl, 2006; Mateu-Vicens et al., 2012), seafloor vegetation allows a wide range of grain sizes to be retained in the proximal region of the shelf. The prevalence of fleshy algae and seagrass close to shore (Figures 2B, 5B & 5D) is the likely reason why any silt-sized grains could be retained in regions of the shelf still affected by some wave activity. As such, the differentiation of the seagrass meadow facies in Malta is more hydrodynamic than compositional as the meadow allows for the retention of a wider range of grain sizes. At present, the distribution of seagrass is highly affected by anthropogenic activities such as coastal development, pollution, trawling, fish farming, moorings, dredging and dumping, leading to an ongoing population change in the community structure (Beca-Carretero et al., 2020; Boudouresque et al., 2009; Telesca et al., 2015). Excluding these impacts, and assuming that salinity and nutrient state on a small region such as the Maltese shelf is relatively uniform, the distribution of this vegetation should be primarily light dependent (Bernardeau-Esteller et al., 2015; Vizzini, 2009). This will limit the distribution of this facies only to the proximal areas and to shallow water as observed here.

Wavelength estimation from wave period (Clifton and Dingler, 1984) based on the data from the Italian RON (Bencivenga et al., 2012) buoy Mazara del Vallo offshore southern Sicily indicate that the maximum wave impact depth (half wavelength, Allen 1985) is at -110 mpsl, this will be considered here as our storm wave base (SWB). Estimation of the fair water wave base (FWWB) is not straightforward, given that there are only around ~30 days of storms and ~60 days of rain a year in Malta (Grabowska 2010), we used the 80% to 90% cumulative frequency cutoff of the mean period to estimate the FWWB at ~ -15mpsl (Figure 3A), as such, most of the sampling occurred

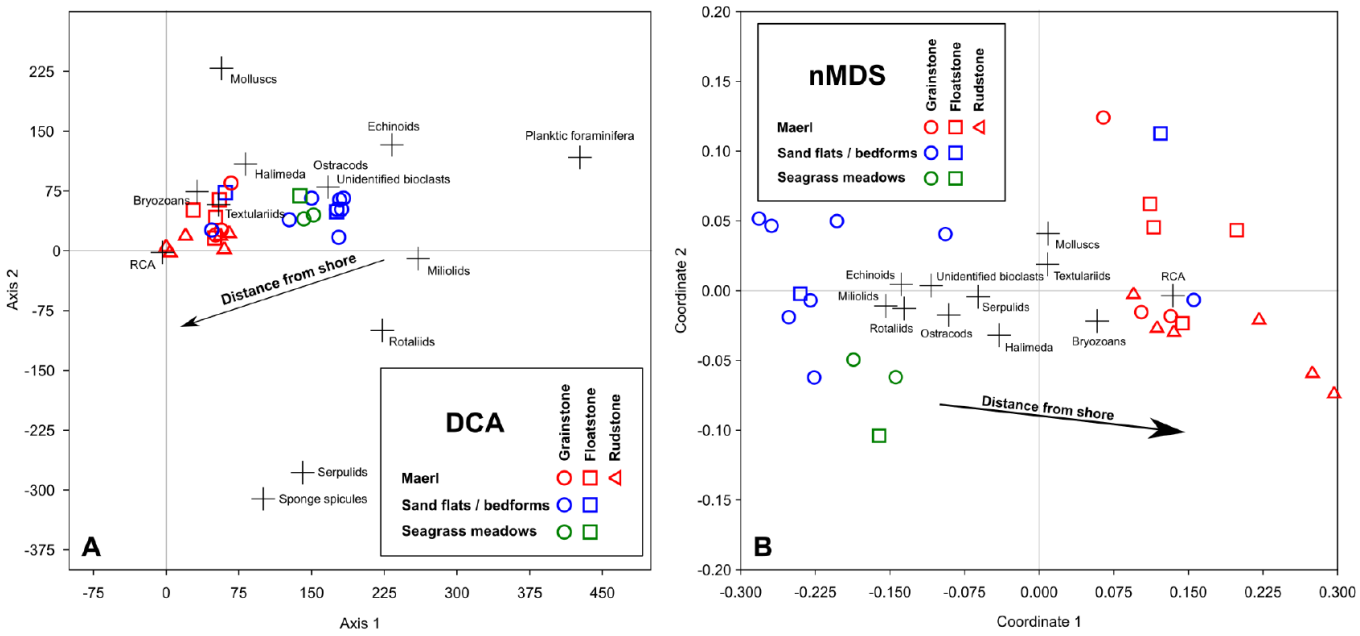

Figure 8: A. DCA and B. nMDS ordination analysis of point counts in thin sections. Both analyses indicate a gradient away from shore.

between the FWWB and SWB (Figure 3B) with representative samples taken from above the FWWB and bellow the SWB.

While the vegetation can explain the retention of fine grain in shallow waters, it does not explain absence of fine grains in deeper water. In this setting fine grains are likely winnowed by two main process: internal waves and bottom currents. Given that the maximum Brunt–Väisälä frequencies (indicating the potential capacity to propagate internal waves) are between ~25 and ~60 mbpsl (Figure 1C) it is unlikely that the winnowing in the outer shelf is dominantly caused by internal waves as the impact of the latter will be focused at the maximum bouncy boundary defined by the high Brunt–Väisälä frequencies. Given that the CTD data were collected in the late summer, when the thermocline is at its deepest (before breaking due to the winter mixing), there is a low probability of this interface occurring at greater depth. That said, pycnocline depth does overlap with the larger sandy bedforms in the mid-shelf (Figure 2B), which are presently below the fair-weather wave base, and is likely a mechanism in shaping them. Although internal waves may explain part of the winnowing on the mid shelf, another cause for the winnowing in the outer shelf is required. The linear arrangements of the rhodolith accumulations would suggest transport along the strike of the shelf, such as would be generated by a contouritic current. The moat at the base of the escarpment (Figure 4) would also support and existence of a shelf parallel bottom current. In the low likelihood of internal waves at this depth, contouritic currents are a more likely mechanism for the winnowing. Such currents would be in line with regional flow regime, notably in summer (Reyes Suarez et al., 2019).

Coralline nodule-rich facies (maerl) are abundant in mesophotic depths in the central Mediterranean (Bracchi and Basso, 2012a; Sañé et al., 2021; Savini et al., 2012). The nature of the facies is variable between individual localities. Moreover, the character of the coralline nodules themselves is highly variable. Across the Maltese shelf they exhibit a wide range of sizes and morphologies as well as amount of live calcareous algal fraction (Sciberras et al., 2009). The specific controls on morphology are not clear. The intermittent growth of the coralline nodules, with termination, reworking and reestablishment (Figure 7o) may be also the result of strong storm events (Dulin et al., 2020). These in turn may impact the transport of the coralline nodules into deeper water. Coralline algae prefer low levels of fines and low light conditions (Coletti et al.,

2018; Leukart and Lüning, 1994; Villas-Bôas et al., 2014). Mediterranean rhodolith beds mainly occur around islands, capes, on the top of submarine plateaus, and in areas influenced by strong tidal currents (Basso et al., 2017). These environments, either due to the lack of clastic input or to currents clearing the sediment, are characterized by a low sedimentation rate. More stable conditions below the main depth interval affected by waves likely leads to the prevalence of this facies in the outer shelf. The dominance of coralline algae in the outer shelf could be also one of the reasons behind the lack of fine-grained material in this domain as well as the abundance of gravel-sized material. Actually, while the seagrass-related facies that dominates close to the coast mainly produce sand-sized material (e.g. Frezza et al., 2011), coralline-algal factories mostly produce coarse-grained bioclasts (e.g. Pomar, 2001). Furthermore, the higher hydrodynamic energy of the coastal sector would promote the fragmentation of bioclasts, resulting in abundant fine-sand-sized material close to the coast. On the other hand, in the outer shelf, characterized by coralline algal facies, the reduced effect of waves, combined with the larger size of the produced bioclasts, would hinder wave-related fragmentation and thus the production of sand and mud sized bioclasts.

Grains derived from *Halimeda* were found in the sediment. However, despite it being reported as a very common algae in the Maltese shelf in the mid-20th century (Larkum et al., 1967), no living *Halimeda* were observed in the AUV, vCTD or grab samples. Interviews carried out with the local diving communities confirm some presence of *Halimeda* on the shelf, but occurrences are rare and in small amount. It is possible that this major contributor has been suppressed in recent years as part of the ongoing species collapse observed in the Mediterranean (Albano et al., 2021; Rilov, 2016). The disparity between *Halimeda* grains presence and living *Halimeda* suggests long retention time of grains in the sedimentary system. This is similarly confirmed by the reworking of coralline nodules and the significant abundance of reworked bioclastic grains across the Maltese shelf. This long retention time may allow for recrystallization, which would account for the high fraction of LMC in the sediment, notably in the outer shelf (Figure 6B).

Controls on sediment and facies distribution on the I/C-type carbonate platform

Energy availability, either from the sun or the breakdown of the organic matter of the ingested food is the main parameter governing and limiting the distribution of carbonate factories on global scale (Bialik et al., 2023). The availability of these two main types of energy is turn related to abiotic parameters such as light availability, water clarity, nutrient abundance, temperature and currents (Halfar et al., 2004; Laugié et al., 2019; Michel et al., 2019; Reijmer, 2021). These parameters also play an important role on smaller scale, together with marine connectivity and local control over sediment transport (Gischler, 2020, 2010, 2006; Jarochowska, 2012; Schmitt and Gischler, 2017). In this regard the Maltese shelf displays similarities with other Mediterranean carbonate systems that are characterized by warm-temperate oligotrophic water (Carannante et al., 1988; Pérès and Picard, 1964). Both the Tyrrhenian shelf (Basso, 1998; Bracchi and Basso, 2012b; Brandano and Civitelli, 2007; Frezza et al., 2011) and the Balearic shelf (Fornós and Ahr, 2006) infralittoral domains are dominated by carbonate factories related to vegetated substrate characterized by abundant epiphytic production. Circalittoral domains are dominated by coralline-algal factories. Further offshore the contribution of pelagic fallout becomes increasingly relevant.

The Maltese shelf differs from the Balearic and Tyrrhenian examples as seagrasses and seaweeds extend to at least 45 mbpsl (Supplements 1, 3) and seagrass-related sediments extend further offshore and further deep. The relevance of carbonate production related to the vegetated substrate can also be observed in the mineralogical composition of the sediment. Notwithstanding the increase in coralline algal abundance moving away from the coast, the HMC fraction decreases. As HMC is essentially related to coralline algae and miliolids and the latter commonly occur as epiphytes (Benedetti and Frezza, 2016; Mateu-Vicens et al., 2012), the

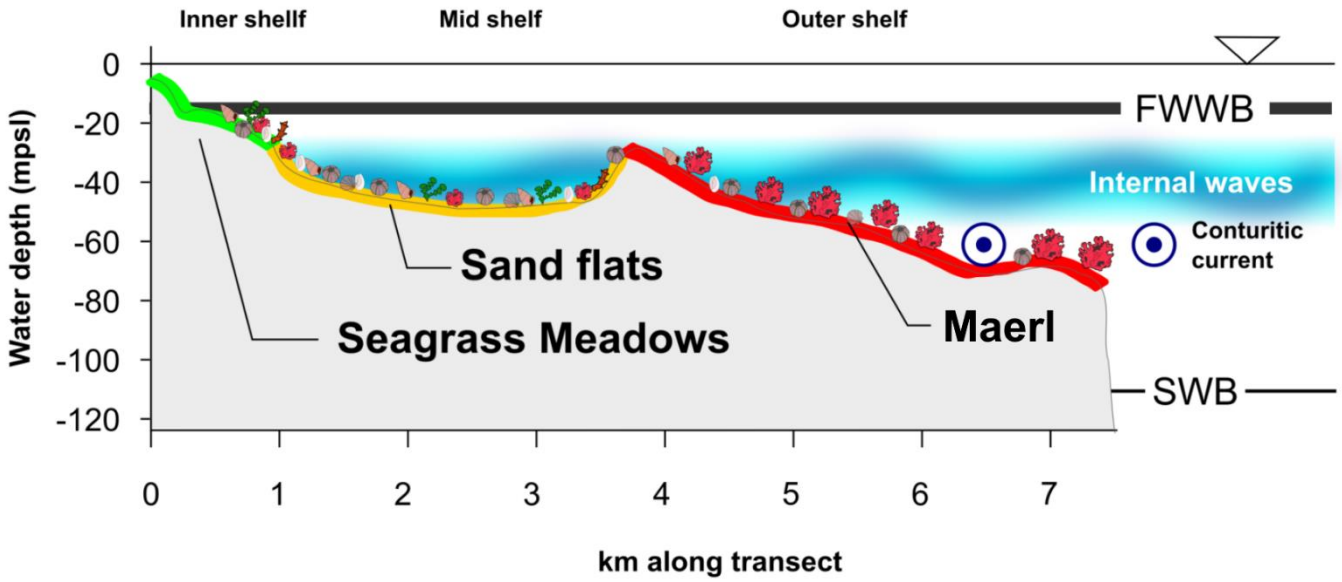

Figure 9: Schematic model of the facies present across the Maltese shelf and main governing parameters on sediment distribution.

decrease of HMC fraction coupled with the increase of coralline algal abundance highlights the importance of epiphytic production along the investigated area of the shelf. The larger extensions of these deposits compared to Balearic and Tyrrhenian location could be caused by the limited siliciclastic supply occurring on the Maltese shelf. As the island is small, mainly consisting of limestone, and is characterized by an arid climate, the terrigenous supply to the shelf is limited. This is also indicated by the LMC fraction in the sediments. As the erosion of Malta's limestone should mainly supply LMC (Gatt, 2021), a significant terrigenous influx from the land should be matched by a peak of LMC close to the coast. This peak is not observed (Figure 6B). Previous authors, based on the overall percentage of carbonate, suggested that most of the carbonate production along the Tyrrhenian and Balearic shelves occur in circalittoral, coralline-algal-dominated, facies (Bracchi and Basso, 2012b; Brandano and Civitelli, 2007). However, as noted by Fornos and Ahr (2006), there is a significant difference between production rates and accumulation rates. Relying only on the latter could be misleading. Furthermore, the percentage of carbonate is the result of both the bioclastic and siliciclastic accumulation rates. Low accumulation rates of siliciclastic detrital material might result in almost pure carbonates even with limited bioclastic production rates. Across the Maltese shelf the abundance of old and reworked material in coralline-algal dominated sediments indicate long exposure of the bioclasts on the seafloor and an overall low accumulation rate. This stresses the need for further studies aimed at assessing accurate accumulation and production rates of both coralline-algal and epiphytic carbonate factories in the Mediterranean and elsewhere.

The relevance of the epiphytic carbonate factory seems to be also one of the main differences that separate the Maltese systems from others dominated by C-type factories like those off Brazil. Similarly to Mediterranean carbonate systems those of the Brazilian coast are characterized by circalittoral production dominated by coralline-algae (Carannante et al., 1988; Testa and Bosence, 1999; Vale et al., 2018). In Brazil, the nearshore settings are usually characterized by a siliciclastic dominated zone, whereas offshore the bioclastic accumulation rates are much higher (Testa and Bosence, 1999). These euphotic carbonate factories are also dominated by *Halimeda*, coralline algae and locally by hermatypic corals. Meanwhile, while seagrass and seaweed meadows are reported (Gomes et al., 2015; Testa and Bosence, 1999) along the Brazilian coast, their prevalence is lower in comparison

to the central Mediterranean. Porcellanaceous foraminifera represent a significant output of these vegetated factories, and may be critical in differentiating between different modes of C-type factories (i.e. Atlantic-like or Mediterranean-like) in geological deposits. Unfortunately, their thin HMC test can be easily dissolved during diagenesis, limiting the possibility of actually recognizing seagrass or seaweed related facies in the fossil record unless other indicators (e.g. large encrusting rotaliids are preserved, Reich et al. 2015; Mariani et al. 2022).

Conclusions

The Maltese shelf is primarily a mesophotic l/C-type carbonate platform. Three main facies could be discerned across the Maltase shelf based on visual inspection (Figure 9): seagrass meadows, sand flats and maerl. However, these facies are not clearly discerned in the sedimentary composition. The sediment along this shelf is dominated by reworked unidentifiable bioclasts associated with coralline algae, benthic foraminifera (notably small miolioliids) and echinoderms. The distribution of these components along the shelf varies but as a gradient rather than clearly discrete spaces. Light and currents (whose effects are in turn controlled by sea-floor morphology) are the main elements governing the facies distribution on the Maltese shelf. Internal waves are mainly relevant on the mid shelf but less so on the outer shelf where contouritic currents are probably more significant. While l/C-type carbonate factories are not prevalent now, these were highly abundant around the Tethys through most of the Cenozoic (Coletti et al., 2022) and these findings should be taken into account into interpreting these environments in the future.

Acknowledgments

The first author is currently supported by Marie Skłodowska Curie fellowship (101003394—RhodoMalta). Ship time was funded by Helmholtz European Partnering project SMART. The surveys were possible following permits issued by the Continental Shelf Department, the Environment and Resources Authority, the Superintendence of Cultural Heritage and the Ports and Yachting Directorate. Supplementary material is available via Figshare as 10.6084/m9.figshare.20330490 (available prior to publication as: https://figshare.com/s/4646c29a9f5d9cc40b2b).

References

Adam, J., Reuther, C.-D., Grasso, M., Torelli, L., 2000. Active fault kinematics and crustal stresses along the Ionian margin of southeastern Sicily. Tectonophysics 326, 217–239. https://doi.org/10.1016/S0040-1951(00)00141-4

Albano, P.G., Steger, J., Bošnjak, M., Dunne, B., Guifarro, Z., Turapova, E., Hua, Q., Kaufman, D.S., Rilov, G., Zuschin, M., 2021. Native biodiversity collapse in the eastern Mediterranean. Proc. R. Soc. B Biol. Sci. 288, 20202469. https://doi.org/10.1098/rspb.2020.2469

Alongi, D.M., 1989. Benthic processes across mixed terrigenous-carbonate sedimentary facies on the central Great Barrier Reef continental shelf. Cont. Shelf Res. 9, 629–663. https://doi.org/10.1016/0278-4343(89)90034-4

Bassi, D., Nebelsick, J.H., 2010. Components, facies and ramps: Redefining Upper Oligocene shallow water carbonates using coralline red algae and larger foraminifera (Venetian area, northeast Italy). Palaeogeogr. Palaeoclimatol. Palaeoecol. 295, 258–280. https://doi.org/10.1016/j.palaeo.2010.06.003

Basso, D., 1998. Deep rhodolith distribution in the Pontian Islands, Italy: a model for the paleoecology of a temperate sea. Palaeogeogr. Palaeoclimatol. Palaeoecol. 137, 173–187. https://doi.org/10.1016/S0031-0182(97)00099-0

Basso, D., Babbini, L., Ramos-Esplá, A.A., Salomidi, M., 2017. Mediterranean rhodolith beds, in: Riosmena-Rodríguez, R., Nelson, W., Aguirre, J. (Eds.), Rhodo- Lith/Maërl Beds: A Global Perspective. Springer, Coastal Research Library 15, pp. 281–299.

Beca-Carretero, P., Teichberg, M., Winters, G., Procaccini, G., Reuter, H., 2020. Projected Rapid Habitat Expansion of Tropical Seagrass Species in the Mediterranean Sea as Climate Change Progresses. Front. Plant Sci. 11. https://doi.org/10.3389/fpls.2020.555376

Ben Ismail, S., Sammari, C., Gasparini, G. Pietro, Béranger, K., Brahim, M., Aleya, L., 2012. Water masses exchanged through the Channel of Sicily: Evidence for the presence of new water masses on the Tunisian side of the channel. Deep Sea Res. Part I Oceanogr. Res. Pap. 63, 65–81. https://doi.org/10.1016/j.dsr.2011.12.009

Bencivenga, M., Nardone, G., Ruggiero, F., Calore, D., 2012. The Italian data buoy network (RON), in: Rahman, M., Brebbia, C.A. (Eds.), Advances in Fluid Mechanics IX. p. 305.

Benedetti, A., Frezza, V., 2016. Benthic foraminiferal assemblages from shallow-water environments of northeastern Sardinia (Italy, Mediterranean Sea). Facies 62, 1–17. https://doi.org/10.1007/s10347-016-0465-9

Bergman, K.L., Westphal, H., Janson, X., Poiriez, A., Eberli, G.P., 2010. Controlling Parameters on Facies Geometries of the Bahamas, an Isolated Carbonate Platform Environment, in: Westphal, H., Riegl, B., Eberli, G.P. (Eds.), Carbonate Depositional Systems: Assessing Dimensions and Controlling Parameters. Springer Netherlands, Dordrecht, pp. 5–80. https://doi.org/10.1007/978-90-481-9364-6_2

Bernardeau-Esteller, J., Ruiz, J.M., Tomas, F., Sandoval-Gil, J.M., Marín-Guirao, L., 2015. Photoacclimation of Caulerpa cylindracea: Light as a limiting factor in the invasion of native Mediterranean seagrass meadows. J. Exp. Mar. Bio. Ecol. 465, 130–141. https://doi.org/10.1016/j.jembe.2014.11.012

Berndt, C., Urlaub, M., Jegen, M., Faghih, Z., Reeck, K., Franz, G., Barnscheidt, K.C., Wollatz-Vogt, M., Liebsch, J., Schramm, B., Elger, J., Kühn, M., Müller, T., Schmidt, M., Spiegel, T., Timm, H., Hinz, A.-K., Sager, T., Hilbert, H.-S., Rohde, L., Korbjuhn, T., Reissmann, S., Diller, N., 2021. RV SONNE Fahrtbericht / Cruise Report SO277 OMAX: Offshore Malta Aquifer Exploration. Keil. https://doi.org/10.3289/GEOMAR_REP_NS_57_20

Bialik, O.M., Coletti, G., Mariani, L., Commissario, L., Desbiolles, F., Meroni, A.N., 2023. Availability and type of energy regulate the global distribution of neritic carbonates. Sci. Rep. 13, 19687. https://doi.org/10.1038/s41598-023-47029-4

Bialik, O.M., Jarochowska, E., Grossowicz, M., 2021. Ordination analysis in sedimentology, geochemistry and palaeoenvironment—Background, current trends and recommendations. Depos. Rec. 7, 541–563. https://doi.org/10.1002/dep2.161

Bialik, O.M., Varzi, A.G., Durán, R., Le Bas, T., Gauci, A., Savini, A., Micallef, A., 2022. Mesophotic Depth Biogenic Accumulations ("Biogenic Mounds") Offshore the Maltese Islands, Central Mediterranean Sea. Front. Mar. Sci. 9. https://doi.org/10.3389/fmars.2022.803687

Biolchi, S., Furlani, S., Antonioli, F., Baldassini, N., Causon Deguara, J., Devoto, S., Di Stefano, A., Evans, J., Gambin, T., Gauci, R., Mastronuzzi, G., Monaco, C., Scicchitano, G., 2016. Boulder accumulations related to extreme wave events on the eastern coast of Malta. Nat. Hazards Earth Syst. Sci. 16, 737–756. https://doi.org/10.5194/nhess-16-737-2016

Bishop, W.F., 1988. Petroleum Geology of East-Central Tunisia. Am. Assoc. Pet. Geol. Bull. 9, 1033–1058.

Bosellini, F.R., Perrin, C., 2008. Estimating Mediterranean Oligocene-Miocene sea-surface temperatures: An approach based on coral taxonomic richness. Palaeogeogr. Palaeoclimatol. Palaeoecol. 258, 71–88. https://doi.org/10.1016/j.palaeo.2007.10.028

Bosence, D.W.J., Pedley, M.H., 1982. Sedimentology and palaeoecology of a Miocene coralline algal biostrome from the Maltese Islands. Palaeogeogr. Palaeoclimatol. Palaeoecol. 38, 9–43. https://doi.org/10.1016/0031-0182(82)90062-1

Boudouresque, C.F., Bernard, G., Pergent, G., Shili, A., Verlaque, M., 2009. Regression of Mediterranean seagrasses caused by natural processes and anthropogenic disturbances and stress: a critical review. botm 52, 395–418. https://doi.org/10.1515/BOT.2009.057

Bracchi, V.A., Basso, D., 2012a. The contribution of calcareous algae to the biogenic carbonates of the continental shelf: Pontian Islands, Tyrrhenian Sea, Italy. Geodiversitas 34, 61–76. https://doi.org/10.5252/g2012n1a4

Bracchi, V.A., Basso, D., 2012b. The contribution of calcareous algae to the biogenic carbonates of the continental shelf: Pontian Islands, Tyrrhenian Sea, Italy. Geodiversitas 34, 61–76.

https://doi.org/10.5252/g2012n1a4

Braga, J.C., Bassi, D., Piller, W.E., 2012. Palaeoenvironmental Significance of Oligocene-Miocene Coralline Red Algae - a Review, in: Mutti, M., Piller, W., Betzler, C. (Eds.), Carbonate Systems during the Oligocene-Miocene Climatic Transition. Wiley-Blackwell, Oxford, UK, pp. 165–182. https://doi.org/10.1002/9781118398364.ch10

Brandano, M., Civitelli, G., 2007. Non-seagrass meadow sedimentary facies of the Pontinian Islands, Tyrrhenian Sea: A modern example of mixed carbonate-siliciclastic sedimentation. Sediment. Geol. 201, 286–301. https://doi.org/10.1016/j.sedgeo.2007.05.012

Carannante, G., Esteban, M., Milliman, J.D., Simone, L., 1988. Carbonate lithofacies as paleolatitude indicators: problems and limitations. Sediment. Geol. 60, 333–346. https://doi.org/10.1016/0037-0738(88)90128-5

Causon Deguara, J., Gauci, R., 2017. Evidence of extreme wave events from boulder deposits on the south-east coast of Malta (Central Mediterranean). Nat. Hazards 86, 543–568. https://doi.org/10.1007/s11069-016-2525-4

Clifton, H.E., Dingler, J.R., 1984. Wave-Formed Structures and Paleoenvironmental Reconstruction. Mar. Geol. 60, 165–198. https://doi.org/10.1016/S0070-4571(08)70146-8

Coletti, G., Basso, D., 2020. Coralline algae as depth indicators in the Miocene carbonates of the Eratosthenes Seamount (ODP Leg 160, Hole 966F). Geobios 60, 29–46. https://doi.org/10.1016/j.geobios.2020.03.005

Coletti, G., Bracchi, V.A., Marchese, F., Basso, D., Savini, A., Vertino, A., Corselli, C., 2018. Quaternary build-ups and rhodalgal carbonates along the adriatic and ionian coasts of the Italian peninsula: A review. Riv. Ital. di Paleontol. e Stratigr. 124, 387–406.

Coletti, G., Commissario, L., Mariani, L., Bosio, G., Desbiolles, F., Soldi, M., Bialik, O.M., 2022. Palaeocene to Miocene southern Tethyan carbonate factories: a meta-analysis of the successions of South-western and Western Central Asia. Depos. Rec. https://doi.org/10.1002/dep2.204

De MacEdo Dias, G.T., Villaa, R.C., 2012. Coralline algae depositional environments on the Brazilian central-south-eastern shelf. J. Coast. Res. 28, 270–279. https://doi.org/10.2112/11T-00003.1

Dulin, T., Avnaim-Katav, S., Sisma-Ventura, G., Bialik, O.M., Angel, D.L., 2020. Rhodolith beds along the southeastern Mediterranean inner shelf: Implications for past depositional environments. J. Mar. Syst. 201, 103241. https://doi.org/10.1016/j.jmarsys.2019.103241

Embry, A.F., Klovan, J.E., 1971. A Late Devonian reef tract on northeastern Banks Island, NWT. Bull. Can. Pet. Geol. 19, 730–781.

Ferraro, L., Innangi, S., Di Martino, G., Russo, B., Tonielli, R., Innangi, M., 2020. Seafloor features and benthic foraminifera off Linosa Island (Sicily Channel, southern Mediterranean). J. Mar. Syst. 211, 103421. https://doi.org/10.1016/j.jmarsys.2020.103421

Fichaut, M., Garcia, M.J., Giorgetti, A., Iona, A., Kuznetsov, A., Rixen, M., Group, M., 2003. MEDAR/MEDATLAS 2002: A Mediterranean and Black Sea database for operational oceanography, in: Dahlin, H., Flemming, N.C., Nittis, K., Petersson, S.E. (Eds.), Building the European Capacity in Operational Oceanography. Elsevier Oceanography Series, Vol. 69, pp. 645–648. https://doi.org/10.1016/S0422-9894(03)80107-1

Flügel, E., 2010. Microfacies of Carbonate Rocks. Springer, Berlin, Heidelberg. https://doi.org/10.1007/978-3-642-03796-2

Foglini, F., Prampolini, M., Micallef, A., Angeletti, L., Vandelli, V., Deidun, A., Soldati, M., Taviani, M., 2016. Late quaternary coastal landscape morphology and evolution of the Maltese Islands (Mediterranean Sea) reconstructed from high-resolution seafloor data. Geol. Soc. Spec. Publ. 411, 77–95. https://doi.org/10.1144/SP411.12

Fonseca, M.S., Koehl, M.A.R., 2006. Flow in seagrass canopies: The influence of patch width. Estuar. Coast. Shelf Sci. 67, 1–9. https://doi.org/10.1016/j.ecss.2005.09.018

Fornós, J.J., Ahr, W.M., 2006. Present-day temperate carbonate sedimentation on the Balearic Platform, western Mediterranean: Compositional and textural variation along a

low-energy isolated ramp. Geol. Soc. Spec. Publ. 255, 71–84. https://doi.org/10.1144/GSL.SP.2006.255.01.06

Frezza, V., Mateu-Vicens, G., Gaglianone, G., Baldassarre, A., Brandano, M., 2011. Mixed carbonate-siliclastic sediments and benthic foraminiferal assemblages from Posidonia oceanica seagrass meadows of the central Tyrrhenian continental shelf (Latium, Italy). Ital. J. Geosci. 130, 352–369. https://doi.org/10.3301/IJG.2011.07

Gaglianone, G., Brandano, M., Mateu-Vicens, G., 2017. The sedimentary facies of Posidonia oceanica seagrass meadows from the central Mediterranean Sea. Facies 63, 1–21. https://doi.org/10.1007/s10347-017-0511-2

Galdies, C., 2011. The Climate of Malta: statistics, trends and analysis 1951-2010. National Statistics Office, Malta, Valleta.

Gatt, P., 2021. Embayment morphometrics, granulometry and carbonate mineralogy of sandy beaches in the Maltese Islands. Mar. Geol. 432, 106394. https://doi.org/10.1016/j.margeo.2020.106394

Gischler, E., 2020. Sediments of the almost-atoll Aitutaki, Cook Islands, South Pacific. Sediment. Geol. 403, 105672. https://doi.org/10.1016/j.sedgeo.2020.105672

Gischler, E., 2010. Sedimentary Facies of Bora Bora, Darwin's Type Barrier Reef (Society Islands, South Pacific): The Unexpected Occurrence of Non-Skeletal Grains. J. Sediment. Res. 81, 1–17. https://doi.org/10.2110/jsr.2011.4

Gischler, E., 2006. Sedimentation on Rasdhoo and Ari Atolls, Maldives, Indian ocean. Facies 52, 341–360. https://doi.org/10.1007/s10347-005-0031-3

Gischler, E., Hudson, J.H., Pisera, A., 2008. Late Quaternary reef growth and sea level in the Maldives (Indian Ocean). Mar. Geol. 250, 104–113. https://doi.org/10.1016/j.margeo.2008.01.004

Gomes, M.P., Vital, H., Eichler, P.P.B., Gupta, B.K.S., 2015. The investigation of a mixed carbonate-siliciclastic shelf, NE Brazil: Side-scan sonar imagery, underwater photography, and surface-sediment data. Ital. J. Geosci. 134, 9–22. https://doi.org/10.3301/IJG.2014.08

Gutscher, M.-A., Dominguez, S., de Lepinay, B.M., Pinheiro, L., Gallais, F., Babonneau, N., Cattaneo, A., Le Faou, Y., Barreca, G., Micallef, A., Rovere, M., 2016. Tectonic expression of an active slab tear from high-resolution seismic and bathymetric data offshore Sicily (Ionian Sea). Tectonics 35, 39–54. https://doi.org/10.1002/2015TC003898

Guy-Haim, T., Silverman, J., Wahl, M., Aguirre, J., Noisette, F., Rilov, G., 2020. Epiphytes provide micro-scale refuge from ocean acidification. Mar. Environ. Res. 161, 105093. https://doi.org/10.1016/j.marenvres.2020.105093

Halfar, J., Eisele, M., Riegl, B., Hetzinger, S., Godinez-Orta, L., 2012. Modern Rhodolith-dominated carbonates at Punta Chivato, Mexico. Geodiversitas 34, 99–113. https://doi.org/10.5252/g2012n1a6

Halfar, J., Godinez-Orta, L., Mutti, M., Valdez-Holguín, J.E., Borges, J.M., 2004. Nutrient and temperature controls on modern carbonate production: An example from the Gulf of California, Mexico. Geology 32, 213. https://doi.org/10.1130/G20298.1

Halfar, J., Mutti, M., 2005. Global dominance of coralline red-algal facies: A response to Miocene oceanographic events. Geology 33, 481–484. https://doi.org/10.1130/G21462.1

Harris, P.M. (Mitch), Purkis, S.J., Ellis, J., Swart, P.K., Reijmer, J.J.G., 2015. Mapping bathymetry and depositional facies on Great Bahama Bank. Sedimentology 62, 566–589. https://doi.org/10.1111/sed.12159

Hendriks, I.E., Bouma, T.J., Morris, E.P., Duarte, C.M., 2010. Effects of seagrasses and algae of the Caulerpa family on hydrodynamics and particle-trapping rates. Mar. Biol. 157, 473–481. https://doi.org/10.1007/s00227-009-1333-8

Hubbard, C.R., Snyder, R.L., 1988. RIR - Measurement and Use in Quantitative XRD. Powder Diffr. 3, 74–77. https://doi.org/10.1017/S0885715600013257

Iuppa, C., Cavallaro, L., Vicinanza, D., Foti, E., 2015. Investigation of suitable sites for wave energy converters around Sicily (Italy). Ocean Sci. 11, 543–557. https://doi.org/10.5194/os-11-543-2015

James, N.P., Bone, Y., Collins, L.B., Kyser, T.K., 2001. Surficial

Sediments of the Great Australian Bight: Facies Dynamics and Oceanography on a Vast Cool-Water Carbonate Shelf. J. Sediment. Res. 71, 549–567. https://doi.org/10.1306/102000710549

Jarochowska, E., 2012. High-resolution microtaphofacies analysis of a carbonate tidal channel and tidally influenced lagoon, Pigeon Creek, San Salvador island, Bahamas. Palaios 27, 151–170. https://doi.org/10.2110/palo.2011.p11-063r

Jongsma, D., van Hinte, J.E., Woodside, J.M., 1985. Geologic structure and neotectonics of the North African Continental Margin south of Sicily. Mar. Pet. Geol. 2, 156–179. https://doi.org/10.1016/0264-8172(85)90005-4

Kiessling, W., Flügel, E., 2002. PALEOREEFS—a database on Phanerozoic reefs, in: Kiessling, W., Flügel, E., Golonka, J. (Eds.), Phanerozoic Reef Patterns. SEPM (Society for Sedimentary Geology), pp. 77–92. https://doi.org/10.2110/pec.02.72.0077

Kiessling, W., Flügel, E., Golonka, J., 1999. Paleoreef Maps: Evaluation of a comprehensive database on Phanerozoic reefs. Am. Assoc. Pet. Geol. Bull. 10, 1552–1587.

Lanfranco, E., Rizzo, M., Hall-Spencer, J., Borg, J.A., Schembri, P.J., 1999. Maerl-forming coralline algae and associated phytobenthos from the Maltese Islands. Cent. Mediterr. Nat. 3.

Larkum, A.W.D., Drew, E.A., Crossett, R.N., 1967. The Vertical Distribution of Attached Marine Algae in Malta. J. Ecol. 55, 361. https://doi.org/10.2307/2257881

Laugié, M., Michel, J., Pohl, A., Poli, E., Borgomano, J., 2019. Global distribution of modern shallow-water marine carbonate factories: a spatial model based on environmental parameters. Sci. Rep. 9, 16432. https://doi.org/10.1038/s41598-019-52821-2

Leukart, P., Lüning, K., 1994. Minimum spectral light requirements and maximum light levels for long-term germling growth of several red algae from different water depths and a green alga. Eur. J. Phycol. 29, 103–112. https://doi.org/10.1080/09670269400650551

Linke, P., Schmidt, M., Rohleder, M., Al-Barakati, A., Al-Farawati, R., 2015. Novel Online Digital Video and High-Speed Data Broadcasting via Standard Coaxial Cable Onboard Marine Operating Vessels. Mar. Technol. Soc. J. 49, 7–18. https://doi.org/10.4031/MTSJ.49.1.2

Lokier, S.W., Al Junaibi, M., 2016. The petrographic description of carbonate facies: are we all speaking the same language? Sedimentology 63, 1843–1885. https://doi.org/10.1111/sed.12293

Mariani, L., Coletti, G., Mateu-Vicens, G., Bosio, G., Collareta, A., Khokhlova, A., Di Cencio, A., Casati, S., Malinverno, E., 2022. Testing an indirect palaeo-seagrass indicator: Benthic foraminifera from the Lower Pleistocene Posidonia meadow of Fauglia (Tuscany, Italy). Mar. Micropaleontol. 173, 102126. https://doi.org/10.1016/j.marmicro.2022.102126

Martin, S., Gattuso, J.-P., 2009. Response of Mediterranean coralline algae to ocean acidification and elevated temperature. Glob. Chang. Biol. 15, 2089–2100. https://doi.org/10.1111/j.1365-2486.2009.01874.x

Mateu-Vicens, G., Brandano, M., Gaglianone, G., Baldassarre, A., 2012. Seagrass-Meadow Sedimentary Facies In A Mixed Siliciclastic-Carbonate Temperate System In the Tyrrhenian Sea (Pontinian Islands, Western Mediterranean). J. Sediment. Res. 82, 451–463. https://doi.org/10.2110/jsr.2012.42

Micallef, A., Georgiopoulou, A., Bas, T. Le, Mountjoy, J.J., Huvenne, V.A.I., Iacono, C. Lo, 2013. Processes on the precipice : seafloor dynamics across the upper Malta-Sicily escarpment, in: Rapport Commission Internationale Mer Méditerranée. Commission Internationale pour l'Exploration Scientifique de la Mer Mediterranee, pp. 39–40.

Micallef, A., Georgiopoulou, A., Mountjoy, J., Huvenne, V.A.I., Iacono, C. Lo, Le Bas, T., Del Carlo, P., Otero, D.C., 2016. Outer shelf seafloor geomorphology along a carbonate escarpment: The eastern Malta Plateau, Mediterranean Sea. Cont. Shelf Res. 131, 12–27. https://doi.org/10.1016/j.csr.2016.11.002

Micallef, A., Le Bas, T.P., Huvenne, V.A.I., Blondel, P., Hühnerbach, V., Deidun, A., 2012. A multi-method approach for benthic habitat mapping of shallow coastal areas with high-resolution multibeam data. Cont. Shelf Res. 39–40, 14–26.

https://doi.org/10.1016/j.csr.2012.03.008

Michel, J., Laugié, M., Pohl, A., Lanteaume, C., Masse, J.-P., Donnadieu, Y., Borgomano, J., 2019. Marine carbonate factories: a global model of carbonate platform distribution. Int. J. Earth Sci. 108, 1773–1792. https://doi.org/10.1007/s00531-019-01742-6

Nalin, R., Basso, D., Massari, F., 2006. Pleistocene coralline algal build-ups (corallige `ne de plateau) and associated bioclastic deposits in the sedimentary cover of Cutro marine terrace (Calabria, southern Italy). Cool. Carbonates Depos. Syst. Palaeoenvironmental Control. 11–22. https://doi.org/10.1144/GSL.SP.2006.255.01.02

Nebelsick, J.H., Bassi, D., 2000. Diversity, growth forms and taphonomy: key factors controlling the fabric of coralline algae dominated shelf carbonates. Geol. Soc. London, Spec. Publ. 178, 89–107. https://doi.org/10.1144/GSL.SP.2000.178.01.07

Osler, J.C., Algan, O., 1999. A high resolution seismic sequence analysis of the Malta Plateau.

Pedley, M.H., Carannante, G., 2006. Cool-water carbonates: Depositional systems and palaeoenvironmental controls. Geol. Soc. London Spec. Publ. 255, 373 pp. https://doi.org/10.1144/GSL.SP.2006.255.01.21

Pérès, J.-M., Picard, J., 1964. Nouveau manuel de bionomie benthique de la mer Méditerranée. Station Marine d'Endoume. Vol 31.

Perrin, C., Bosellini, F.R., 2012. Paleobiogeography of scleractinian reef corals: Changing patterns during the Oligocene–Miocene climatic transition in the Mediterranean. Earth-Science Rev. 111, 1–24. https://doi.org/10.1016/j.earscirev.2011.12.007

Placenti, F., Schroeder, K., Bonanno, A., Zgozi, S., Sprovieri, M., Borghini, M., Rumolo, P., Cerrati, G., Bonomo, S., Genovese, S., Basilone, G., Haddoud, D.A., Patti, B., El Turki, A., Hamza, M., Mazzola, S., 2013. Water masses and nutrient distribution in the Gulf of Syrte and between Sicily and Libya. J. Mar. Syst. 121–122, 36–46. https://doi.org/10.1016/j.jmarsys.2013.03.012

Pomar, L., Baceta, J.I., Hallock, P., Mateu-Vicens, G., Basso, D., 2017. Reef building and carbonate production modes in the west-central Tethys during the Cenozoic. Mar. Pet. Geol. 83, 261–304. https://doi.org/10.1016/j.marpetgeo.2017.03.015

Pomar, L., Kendall, C.G.S.C., 2008. Architecture of Carbonate Platforms: A Response to Hydrodynamics and Evolving Ecology, in: Lukasik, J., Simo, J.A. (Eds.), Controls on Carbonate Platform and Reef Development. SEPM Spacial Publication 89, pp. 187–216. https://doi.org/10.2110/pec.08.89.0187

Prampolini, M., Blondel, P., Foglini, F., Madricardo, F., 2018. Habitat mapping of the Maltese continental shelf using acoustic textures and bathymetric analyses. Estuar. Coast. Shelf Sci. 207, 483–498. https://doi.org/10.1016/j.ecss.2017.06.002

Prampolini, M., Foglini, F., Biolchi, S., Devoto, S., Angelini, S., Soldati, M., 2017. Geomorphological mapping of terrestrial and marine areas, northern Malta and Comino (central Mediterranean Sea). J. Maps 13, 457–469. https://doi.org/10.1080/17445647.2017.1327507

Rasband, W., Contributors, 2021. ImageJ 1.53e.

Rasser, M.W., 2000. Coralline red algal limestones of the late Eocene alpine Foreland Basin in Upper Austria: Component analysis, facies and palecology. Facies 42, 59–92. https://doi.org/10.1007/BF02562567

Reich, S., Di Martino, E., Todd, J.A., Wesselingh, F.P., Renema, W., 2015. Indirect paleo-seagrass indicators (IPSIs): A review. Earth-Science Rev. 143, 161–186. https://doi.org/10.1016/j.earscirev.2015.01.009

Reijmer, J.J.G., 2021. Marine carbonate factories: Review and update. Sedimentology 68, 1729–1796. https://doi.org/10.1111/sed.12878

Reuther, C.-D., Ben-Avraham, Z., Grasso, M., 1993. Origin and role of major strike-slip transfers during plate collision in the central Mediterranean. Terra Nov. 5, 249–257. https://doi.org/10.1111/j.1365-3121.1993.tb00256.x

Reyes Suarez, Cook, Gačić, Paduan, Drago, Cardin, 2019. Sea Surface Circulation Structures in the Malta-Sicily Channel from Remote Sensing Data. Water 11, 1589. https://doi.org/10.3390/w11081589

Rilov, G., 2016. Multi-species collapses at the warm edge of a warming sea. Sci. Rep. 6, 36897. https://doi.org/10.1038/srep36897

Rindi, F., Braga, J.C., Martin, S., Peña, V., Le Gall, L., Caragnano, A., Aguirre, J., 2019. Coralline Algae in a Changing Mediterranean Sea: How Can We Predict Their Future, if We Do Not Know Their Present? Front. Mar. Sci. 6. https://doi.org/10.3389/fmars.2019.00723

Sañé, E., Ingrassia, M., Chiocci, F.L., Argenti, L., Martorelli, E., 2021. Characterization of rhodolith beds-related backscatter facies from the western Pontine Archipelago (Mediterranean Sea). Mar. Environ. Res. 169, 105339. https://doi.org/10.1016/j.marenvres.2021.105339

Savini, A., Basso, D., Alice Bracchi, V., Corselli, C., Pennetta, M., 2012. Maerl-bed mapping and carbonate quantification on submerged terraces offshore the Cilento peninsula (Tyrrhenian Sea, Italy). Geodiversitas 34, 77–98. https://doi.org/10.5252/g2012n1a5

Schlager, W., 2005. Carbonate Sedimentology and Sequence Stratigraphy. SEPM concepts in sedimentology and paleontology, volume 8, Tulsa, Oklahoma. https://doi.org/10.2110/csp.05.08

Schlager, W., 2003. Benthic carbonate factories of the Phanerozoic. Int. J. Earth Sci. 92, 445–464. https://doi.org/10.1007/s00531-003-0327-x

Schmitt, D., Gischler, E., 2017. Recent sedimentary facies of Roatan (Bay Islands, Honduras), a Caribbean oceanic barrier reef system. Facies 63, 5. https://doi.org/10.1007/s10347-016-0485-5

Sciberras, M., Rizzo, M., Mifsud, J.R., Camilleri, K., Borg, J.A., Lanfranco, E., Schembri, P.J., 2009. Habitat structure and biological characteristics of a maerl bed off the northeastern coast of the Maltese Islands (central Mediterranean). Mar. Biodivers. 39, 251–264. https://doi.org/10.1007/s12526-009-0017-4

Smith, T.B., Frankel, E., Jell, J.S., 1998. Lagoonal sedimentation and reef development on Heron Reef, southern Great Barrier Reef province, in: Reefs and Carbonate Platforms in the Pacific and Indian Oceans. pp. 281–294.

Telesca, L., Belluscio, A., Criscoli, A., Ardizzone, G., Apostolaki, E.T., Fraschetti, S., Gristina, M., Knittweis, L., Martin, C.S., Pergent, G., Alagna, A., Badalamenti, F., Garofalo, G., Gerakaris, V., Louise Pace, M., Pergent-Martini, C., Salomidi, M., 2015. Seagrass meadows (Posidonia oceanica) distribution and trajectories of change. Sci. Rep. 5, 12505. https://doi.org/10.1038/srep12505

Testa, V., Bosence, D.W.J., 1999. Physical and biological controls on the formation of carbonate and siliciclastic bedforms on the north-east Brazilian shelf. Sedimentology 46, 279–301. https://doi.org/10.1046/j.1365-3091.1999.00213.x

Tucker, M.E., Wright, V.P., 1990. Carbonate Sedimentology. Blackwell Publishing Ltd., Oxford, UK. https://doi.org/10.1002/9781444314175

UNESCO, 1981. Tenth report of the joint panel on oceanographic tables and standards. Unesco technical papers in marine science, Vol. 36.

Vale, N.F., Amado-Filho, G.M., Braga, J.C., Brasileiro, P.S., Karez, C.S., Moraes, F.C., Bahia, R.G., Bastos, A.C., Moura, R.L., 2018. Structure and composition of rhodoliths from the Amazon River mouth, Brazil. J. South Am. Earth Sci. 84, 149–159. https://doi.org/10.1016/j.jsames.2018.03.014

Vallis, G.K., 2017. Atmospheric and Oceanic Fluid Dynamics - Fundamentals and Large-Scale Circulation. Cambridge University Press, Cambridge, UK. https://doi.org/10.1017/9781107588417

Villas-Bôas, A.B., Tâmega, F.T.D.S., Andrade, M., Coutinho, R., Figueiredo, M.A.D.O., 2014. Experimental Effects of Sediment Burial and Light Attenuation on Two Coralline Algae of a Deep Water Rhodolith Bed in Rio de Janeiro, Brazil. Cryptogam. Algol. 35, 67–76. https://doi.org/10.7872/crya.v35.iss1.2014.67

Vizzini, S., 2009. Analysis of the trophic role of Mediterranean seagrasses in marine coastal ecosystems: a review. Bot. Mar. 52, 383–393. https://doi.org/10.1515/BOT.2009.056

Warn-Varnas, A., Sellschopp, J., Haley, P.., Leslie, W.., Lozano, C.., 1999. Strait of Sicily water masses. Dyn. Atmos. Ocean. 29, 437–469. https://doi.org/10.1016/S0377-0265(99)00014-7

Westphal, H., Halfar, J., Freiwald, A., 2010. Heterozoan carbonates in subtropical to tropical settings in the present and past. Int. J. Earth Sci. 99, 153–169. https://doi.org/10.1007/s00531-010-0563-9